Int. J. Solids Structures Vol. 30, No. 9, pp. 1269–1288, 1993
Printed in Great Britain

0020–7683/93 $6.00+ .00

YIELD CRITERION AND LOADING FUNCTION FOR CONCRETE PLASTICITY

MONDHER LABBANE, NRIPENDRA K. SAHA† and EDWARD C. TING
School of Civil Engineering, Purdue University, West Lafayette, IN 47907, U.S.A.

(*Received* 20 *June* 1991; *in revised form* 17 *August* 1992)

Abstract—The findings of our continuing efforts during the last decade to develop a rational plasticity-based numerical model for the response and failure prediction of reinforced concrete structures are summarized. Several plasticity-fracture models are implemented in two general purpose finite element codes to evaluate the effect of yield criterion and loading function selections. Four sets of experimental data were considered in the comparative study. The significance of properly modeled loading functions is illustrated by homogeneous deformations as well as two reinforced concrete structural problems. Accurate modeling of stress–strain relationships is shown to be of critical importance in the prediction of concrete structural failure.

1. INTRODUCTION

During recent years, considerable attention has been focused on the computational analysis of reinforced concrete structures. A critical area of concern is the development of a suitable concrete model including the constitutive relation that characterizes the behavior of concrete prior to fracture. Considering the wide variability in the concrete ingredients and the experimental data, skepticism has often been raised as to whether the behavior of concrete can be formulated by a rational continuum approach. A variety of studies have given promising signs that the mechanical behavior of concrete structures can be reasonably predicted from the knowledge of quality control tests. However, satisfactory concrete constitutive relations which have the capability of predicting general concrete structural behaviors are not available at this time.

Different approaches have been proposed for the numerical modeling of concrete. The commonly used models are the linear and nonlinear elastic models and the work-hardening plastic models. Elasticity-based models employ a linear, bilinear or nonlinear law for isotropic or anisotropic materials in conjunction with a fracture criteria. This approach has the advantage of simplicity and ease of numerical implementation. However, the elasticity-based models are limited in applications. For example, they lack the mechanism to represent the important irreversible concrete behavior. To circumvent such a shortcoming in a rational and efficient manner, plasticity-based models have been proposed to describe the physical nonlinearity and the irreversible behavior. However, in spite of the proliferation of plasticity-based models, a careful review indicates that many of these models have not been critically validated as to their accuracy and suitability to predict concrete behavior. The present paper is an attempt to study the yield criterion and the subsequent loading function in a plastic flow theory, which is a critical element of the concrete plasticity.

Most of the plasticity-based concrete models proposed follow the classical plasticity theories developed for metals. Thus, the primary elements of the models are the yielding functions and the hardening laws which physically model the initiation and progress of microcracking phenomenon in the concrete medium. For convenience and consistency, an important assumption in nearly all the concrete plasticity formulations is that the yielding and subsequent loading functions have the same functional form as the fracture criterion, thus satisfying compatibility at the point of failure. The first objective of this study is then to examine the accuracy of this pivotal assumption based on biaxial and triaxial data. Such a careful scrutiny is necessary since experimental observation indicates that concrete yielding due to internal slip and microcrack growth and concrete failure due to brittle fracture are

† Currently with Ford Motor Company.

physically different phenomena. In the subsequent study, we consider the use of different functional forms for the yield surface, loading surface and fracture surface. Some combinations are implemented in finite element codes for plane problems and plate analysis. Using benchmark stress analysis problems, the differences in using different yield and loading functions are demonstrated.

A large number of functional forms have been proposed in the literature to describe concrete fracture surfaces. Most of the functions are formulated based on biaxial test data only. In this study, five functions are selected for evaluation of yielding and work hardening; namely the functions proposed by (1) von Mises, (2) Drucker and Prager (1952), (3) Hsieh *et al.* (1982), (4) Willam and Warnke (1974) and (5) Bresler and Pister (1958). The Drucker and Prager and Bresler and Pister functions were proposed based on biaxial fracture data. Functions proposed by Hsieh *et al.* and Willam and Warnke are more general models based on both the biaxial and triaxial fracture data.

To study the effect of plasticity yield criterion and loading functions on the overall behavior of concrete structures, a concrete fracture surface that serves as the bounding surface for the plasticity-based concrete stress–strain response must be proposed. For this purpose, a fracture surface of the same shape as the yield surface is used in the Hsieh *et al.* and Willam and Warnke models. Plasticity theories using the other three models are bounded by the Hsieh *et al.* fracture envelope.

2. YIELD CRITERIA AND LOADING FUNCTIONS FOR CONCRETE PLASTICITY

Failure criteria functions for concrete can be expressed in the following form:

$$f(I_1, J_2, J_3, f'_c) = 0, \tag{1}$$

where

I_1 = the first stress invariant,
$I_1 = \sigma_1+\sigma_2+\sigma_3$,
J_2 = the second deviatoric stress invariant,
$J_2 = \frac{1}{6}[(\sigma_1-\sigma_2)^2+(\sigma_2-\sigma_3)^2+(\sigma_3-\sigma_1)^2]$,
J_3 = the third deviatoric stress invariant,
$J_3 = s_1 s_2 s_3$,
$\sigma_1, \sigma_2, \sigma_3$ = principal stresses,
s_1, s_2, s_3 = principal deviatoric stresses,
f'_c = uniaxial compressive fracture strength of concrete obtained from the control test.

The functions are proposed based on fracture test data. To obtain the initial yielding and subsequent loading functions for concrete stress–strain relationships, f'_c is often replaced by a hardening parameter τ, which measures the size of the loading surface

$$f(I_1, J_2, J_3, \tau) = 0. \tag{2}$$

Thus, the yield criterion and the loading functions are expressed in the same form as the fracture criterion. A value of 25–35% of the uniaxial compressive strength is commonly assumed as the initial concrete yield strength.

2.1. *von Mises function*

The von Mises function is widely used in metal plasticity. The function depends on only one stress invariant and does not include the effect of hydrostatic stresses. It has the following form:

$$\sqrt{3J_2}-\tau = 0. \tag{3}$$

2.2. *Drucker–Prager function*

The Drucker–Prager function is a modification of the von Mises function. It includes the effect of hydrostatic stresses by adding another stress invariant to the von Mises function

$$\alpha I_1+\beta\sqrt{J_2}-\tau = 0, \tag{4}$$

where α and β are material constants.

The material constants can be determined from two fracture states, such as:

—uniaxial compressive strength: $\sigma_1 = \sigma_2 = 0, \sigma_3 = -f'_c$,
—equal biaxial strength: $\sigma_1 = 0, \sigma_2 = \sigma_3 = -f'_{bc}$.

If $f'_{bc} = 1.15, f'_c$ is used, the two constants are found to be:

$$\alpha = 0.1304, \quad \beta = 1.9580. \tag{5}$$

2.3. *Hsieh–Ting–Chen function*

Hsieh *et al.* proposed a four parameter failure criterion that defines the ultimate strength of concrete. By proportionally scaling down the fracture surface, the following loading function is obtained

$$A\frac{J_2}{\tau^2}+B\frac{\sqrt{J_2}}{\tau}+C\frac{\sigma_1}{\tau}+D\frac{I_1}{\tau}-1 = 0, \tag{6}$$

where σ_1 is the maximum principal stress.

The parameters A, B, C and D are nondimensional material constants to be determined from the fracture data. It is interesting to note that the four parameter criterion is a linear combination of simpler criteria. The function reduces to the von Mises criterion when A, C and D are set equal to zero, and to the Drucker–Prager criterion when A and D are equal to zero.

To determine the function parameters, four fracture states are considered:

—uniaxial tensile strength: $\sigma_1 = f'_t, \sigma_2 = \sigma_3 = 0$,
—uniaxial compressive strength: $\sigma_1 = \sigma_2 = 0, \sigma_3 = -f'_c$,
—equal biaxial strength: $\sigma_1 = 0, \sigma_2 = \sigma_3 = -f'_{bc}$,
—confined triaxial compressive strength: $\sigma_1 = \sigma_2 = -f'_{pc}, \sigma_3 = -f'_{cc}$.

If the following values are assumed:

$$f'_t = 0.10f'_c, \quad f'_{bc} = 1.15f'_c, \quad f'_{pc} = 0.8f'_c, \quad f'_{cc} = 4.2f'_c,$$

the material constants are found to be:

$$A = 2.0108, \quad B = 0.9714, \quad C = 9.1412, \quad D = 0.2312.$$

2.4. *Willam–Warnke function*

Willam and Warnke suggested a failure criterion that involves five parameters. This criterion has a complicated form; however, it represents a smooth envelope and has a unique gradient value everywhere. It accurately defines the ultimate strength of concrete in all stress regions. The Willam and Warnke criterion has the following form:

$$\sqrt{5}\tau_m - r = 0, \tag{7}$$

where

$$r = \frac{2r_c(r_c^2 - r_t^2)\cos\theta + r_c(2r_t - r_c)\sqrt{4(r_c^2 - r_t^2)\cos^2\theta + 5t_t^2 - 4r_t r_c}}{4(r_c^2 - r_t^2)\cos^2\theta + (r_c - 2r_t)^2}, \tag{8}$$

$$r_t = \sqrt{5}\tau\left[a_0 + a_1\left(\frac{\sigma_m}{\tau}\right) + a_2\left(\frac{\sigma_m}{\tau}\right)^2\right], \tag{9}$$

$$r_c = \sqrt{5}\tau\left[b_0 + b_1\left(\frac{\sigma_m}{\tau}\right) + b_2\left(\frac{\sigma_m}{\tau}\right)^2\right], \tag{10}$$

$$\tau_m = \sqrt{\tfrac{2}{5}J_2}, \tag{11}$$

$$\sigma_m = \tfrac{1}{3}I_1. \tag{12}$$

The six constants a_0, a_1, a_2, b_0, b_1 and b_2 required in the Willam–Warnke function can be found from three standard concrete tests and two strength tests in triaxial compression, in addition to the condition that both tensile and compressive meridians must intersect the hydrostatic axis at a common point.

To determine the function parameters, five fracture states are considered:

—uniaxial tensile strength: $\sigma_1 = f'_t$, $\sigma_2 = \sigma_3 = 0$,
—uniaxial compressive strength: $\sigma_1 = \sigma_2 = 0$, $\sigma_3 = -f'_c$,
—equal biaxial strength: $\sigma_1 = 0$, $\sigma_2 = \sigma_3 = -f'_{bc}$,
—confined triaxial compressive strength (compressive meridian): $\sigma_m = -\sigma_{mc}$, $r = r_c$,
—confined triaxial compressive strength (tensile meridian): $\sigma_m = -\sigma_{mt}$, $r = r_t$.

If the following values are assumed:

$$f'_t = 0.10f'_c, \quad f'_{bc} = 1.15f'_c, \quad \sigma_{mc} = 1.95f'_c,$$
$$r_c = 2.77f'_c, \quad \sigma_{mt} = 3.67f'_c, \quad r_t = 1.40f'_c,$$

the material constants are found:

$$a_0 = 0.05347, \quad a_1 = -0.50731, \quad a_2 = -0.03826,$$
$$b_0 = 0.09217, \quad b_1 = -0.86653, \quad b_2 = -0.14283.$$

2.5. *Bresler–Pister function*

The Bresler–Pister loading function is expressed in terms of the octahedral shearing stress τ_{oct}, and the octahedral normal stress σ_{oct}:

$$\frac{\tau_{oct}}{\tau} + B\frac{\sigma_{oct}}{\tau} - C\left(\frac{\sigma_{oct}}{\tau}\right)^2 = A. \tag{13}$$

The constants A, B and C can be determined from the following three fracture states:

—uniaxial tensile strength: $\sigma_1 = f'_t$, $\sigma_2 = \sigma_3 = 0$,
—uniaxial compressive strength: $\sigma_1 = \sigma_2 = 0$, $\sigma_3 = -f'_c$,
—equal biaxial strength: $\sigma_1 = 0$, $\sigma_2 = \sigma_3 = -f'_{bc}$.

Assuming the following values:

$$f'_t = 0.10f'_c, \quad f'_{bc} = 1.15f'_c,$$

the material constants are found to be:

$$A = 0.098, \quad B = 1.530, \quad C = -1.240.$$

3. EVALUATION OF LOADING FUNCTIONS

To evaluate the loading functions considered in this study, two different sets of biaxial test data and two sets of triaxial data are used. The evaluation process consists of two parts. First, the test data for different loading conditions are utilized to compute the hardening parameter τ as a function of the effective plastic strain ε_p which is given by

$$\varepsilon_p = \int \sqrt{d\varepsilon_{ij}^p \, d\varepsilon_{ij}^p}, \tag{14}$$

where $d\varepsilon_{ij}^p$ is the plastic strain increment. The τ vs ε_p curves of a particular loading function evaluated for different stress combinations should merge into a single curve. That is, a unique hardening function should be able to describe the strain hardening behavior regardless of the loading conditions. The second part of the evaluation includes the complete elastic–plastic constitutive equation. Using the yield and loading functions under consideration and the parameters determined from the test data, the accuracy of the prediction of concrete stress–strain behavior is tested for each model.

The evaluation study is carried out separately for the biaxial and the triaxial conditions.

3.1. *Evaluation based on the biaxial test data*

The biaxial test data reported by Kupfer *et al.* (1969) are first utilized. Figure 1 plots the normalized hardening parameter (τ/f'_c) vs the effective plastic strain (ε_p) for the presently considered loading functions. For the von Mises functions, the hardening curves under different loading conditions merge into a single curve, thus satisfying the uniqueness condition of the hardening parameter. Under uniaxial tension and compression–tension states of stress, the value of τ/f'_c fails to reach 1.0. This is due to the cut-off failure surface that bounds all loading functions. On the other hand, under equal biaxial compression the value

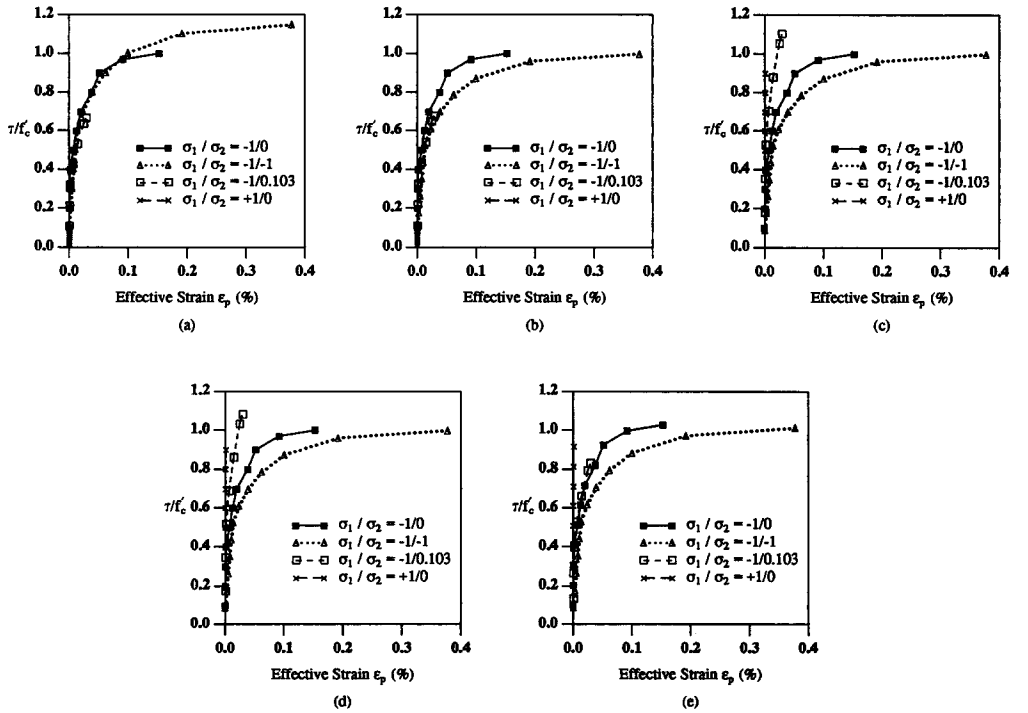

Fig. 1. Biaxial hardening parameter for different choices of loading functions based on Kupfer data: (a) von Mises, (b) Drucker–Prager, (c) Hsieh–Ting–Chen, (d) Willam–Warnke, and (e) Bresler–Pister.

of τ/f'_c is seen to approach 1.15. This is because the von Mises functions do not predict an increase in strength under equal biaxial compression. Thus, if the normalized hardening is selected to be less than 1.0 under all loading conditions, this will lead to a perfect state of plasticity at an equal biaxial compression of f'_c, and the fracture surface will not be reached. By introducing the effect of hydrostatic stresses, the Drucker–Prager functions eliminate this important flaw. As can be seen from Fig. 1(b), all curves remain under 1.0 for the loading conditions considered. Moreover, the curves exhibit a good uniformity of slope under various loading conditions.

Figures 1(c) and (d) show that the hardening functions for the Hsieh *et al.* and the Willam and Warnke loading functions exhibit essentially the same characteristics. Since the same functional form is used for the loading and fracture surfaces, the ratio τ/f'_c approaches 1.0 for all loading conditions, except for the tension–compression case where it exceeds 1.0. This is because both the Hsieh *et al.* and Willam and Warnke slightly underestimate the failure strength under this loading condition, based on Kupfer data. More importantly, however, the hardening curves show widely varying slopes under various loading combinations. The hardening rate is highest in uniaxial tension, and smallest in biaxial compression. Hence, if the standard compression curve is used to characterize the hardening behavior, the two functions predict a response that is much too soft in tension and too stiff in biaxial compression.

Hardening curves for the Bresler–Pister loading functions are shown in Fig. 1(e). These curves exhibit a trend similar to that of the Hsieh *et al.* and Willam–Warnke functions. Thus, under biaxial loading, a similar response is expected.

To further confirm the above findings, another set of biaxial test data reported by Tasuji *et al.* (1978) is used. The characteristics of the hardening parameters evaluated on the basis of Tasuji data are essentially the same as those exhibited by the hardening parameters based on Kupfer data.

Based on the first part of the evaluation process, it appears that the assumption of using yielding and loading functions of the same form as the fracture criterion is not generally valid. Loading functions based on this assumption tend to predict hardening parameters with widely varying rates. The von Mises or the Drucker–Prager functions seem to be better suited in a plasticity-based constitutive formulation in the absence of large hydrostatic pressure.

In the second part of our evaluation process, the stress–strain behavior due to homogeneous deformations is analysed using a single concrete finite element. The corresponding hardening parameter is determined from the uniaxial compressive data. Since, all the loading functions exhibit the same hardening curves under uniaxial compression, the same curve is used for all models. Through a simple regression analysis, the following relation is obtained:

$$\frac{\tau}{f'_c} = 1.0 - 0.75\, e^{-2650\varepsilon_p} \tag{15}$$

and the corresponding hardening rate is then

$$H = \frac{\partial \tau}{\partial \varepsilon_p} = 1988 f'_c\, e^{-2650\varepsilon_p}. \tag{16}$$

The hardening curve given by eqn (15) is compared to the experimental data in Fig. 2, for the von Mises and Drucker–Prager loading functions. Data plots for other functional choices show a much wider scattering.

Figures 3–5 show comparisons of the predicted stress–strain relationships with Kupfer data under various loading conditions. Under uniaxial compression, good agreement is exhibited for all choices of loading functions, with a slightly better performance from the von Mises and Drucker–Prager functions. This result is expected as the hardening parameter

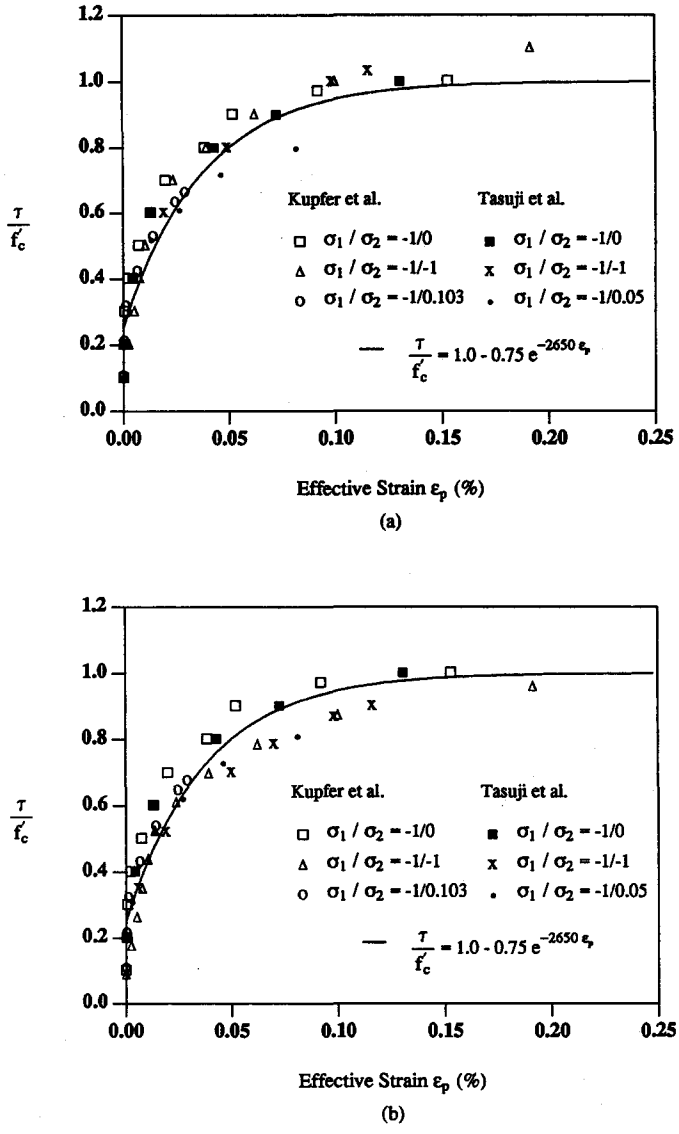

Fig. 2. Data: (a) von Mises and (b) Drucker–Prager.

is characterized from the uniaxial compression test data. Figure 3(b) compares predictions under equal biaxial compression states of stress. The von Mises loading functions yield accurate predictions until the equal biaxial stresses reach f'_c, when the strains become indefinitely large. As explained earlier, this is due to the inability of the von Mises functions to predict the increased strength under biaxial compressive stresses. The Drucker–Prager functions exhibit good agreement with the experimental data, but slightly overestimate the concrete stiffness at higher strain levels. For the Hsieh *et al.* and Willam–Warnke functions, larger discrepancies are observed. Figure 3(c) shows the stress–strain relations under biaxial compression for the principal stress ratio σ_1/σ_2 of $-1/-0.5$. Similar results to the equal biaxial compression case are observed.

Figure 4 shows the stress–strain predictions under tension–compression states of stress. The von Mises and Drucker–Prager yield excellent agreement for all stress ratios. For the Hsieh *et al.* and Willam–Warnke functions, while the major principal compressive strains are accurately predicted, great discrepancies can be observed between the calculated and measured tensile strain values in the direction of the minor principal strain. Under uniaxial

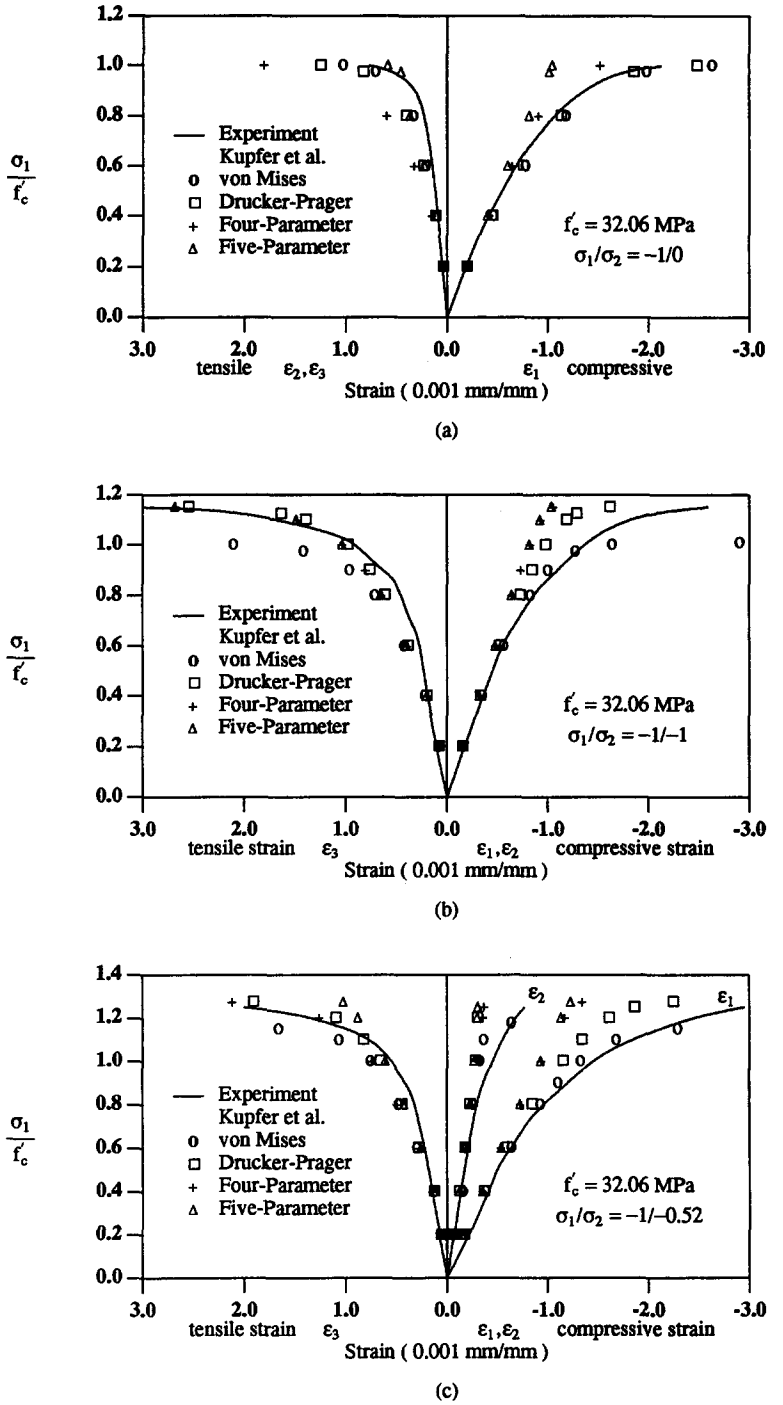

Fig. 3. Formulations: (a) uniaxial compression, (b) equal biaxial compression, and (c) unequal biaxial compression.

and biaxial tension, the discrepancies between the predicted and experimental strain values are even larger, as can be seen from Fig. 5. Good agreement is again achieved by the von Mises and Drucker–Prager functions.

To further validate the above results, Tasuji data are again used for comparisons (Labbane *et al.*, 1991). Despite using different mix designs and laboratory equipment, similar trends are observed, thus confirming the findings based on Kupfer data.

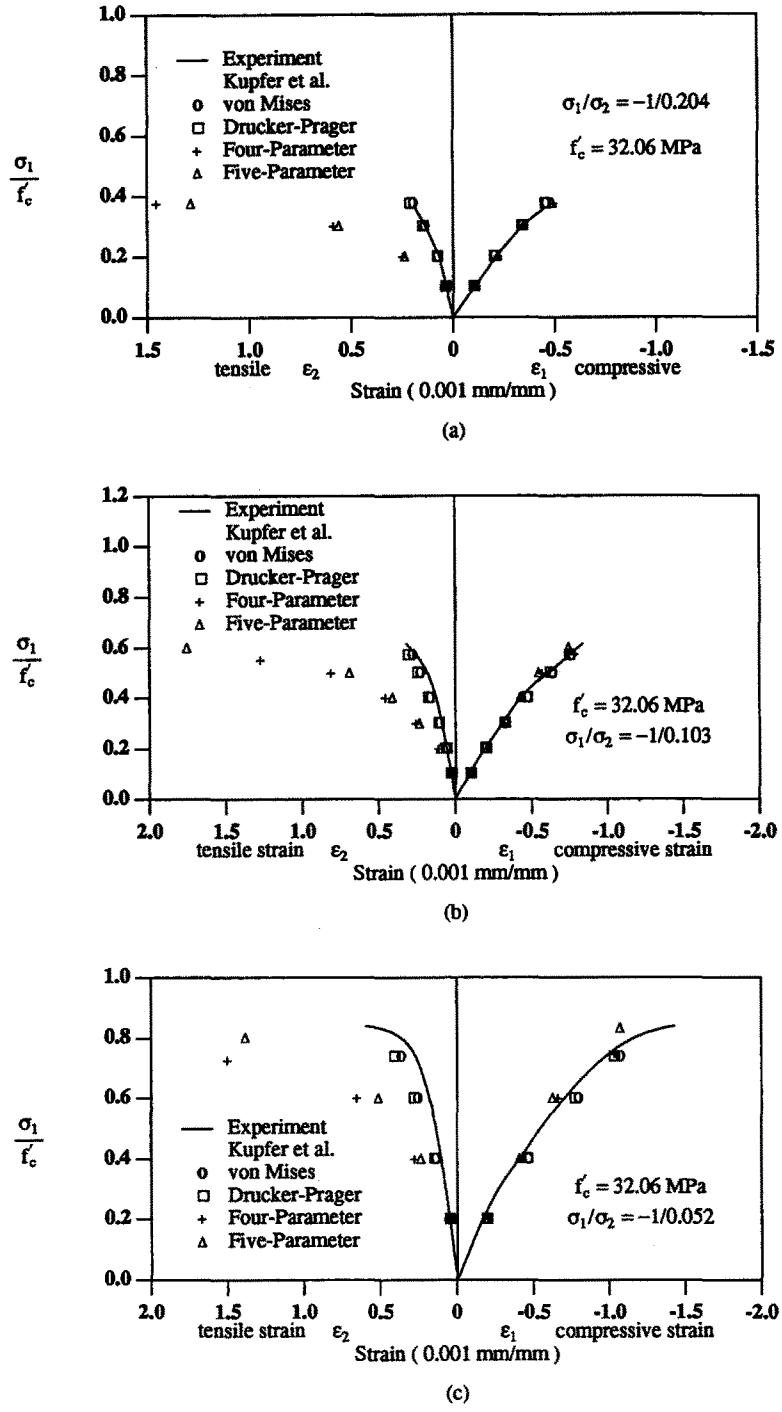

Fig. 4. Tensile–compressive stress–strain behavior of concrete plasticity formulations under three different stress ratios.

On the basis of the analytical results discussed above, loading functions that heavily include the effects of hydrostatic pressure tend to yield very poor predictions of the stress–strain relations, particularly the tensile strains. Both the Hsieh *et al.* and the Willam–Warnke loading functions predict a considerably softer response for tensile loading while in biaxial compression both criteria have a stiffer response. Suppressing or minimizing the effect of hydrostatic stresses as in the von Mises and Drucker–Prager functions greatly

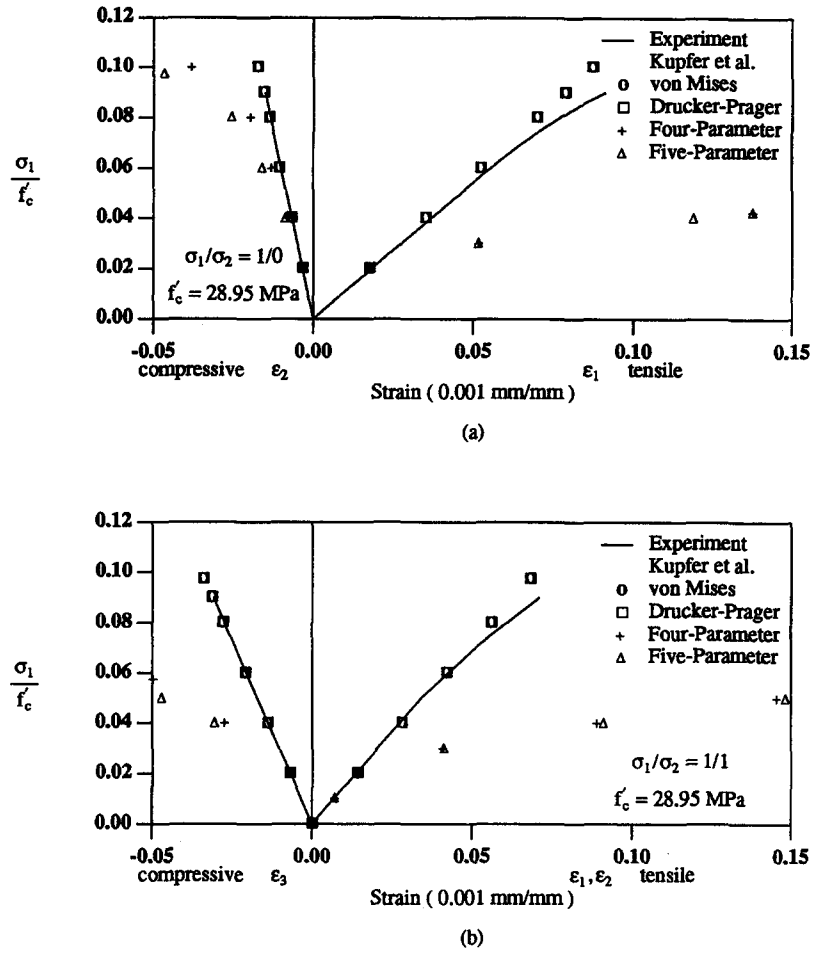

Fig. 5. Tensile stress–strain behavior of concrete plasticity formulations: (a) uniaxial tension, and (b) equal biaxial tension.

improves the predictions. Both functions achieve similarly accurate predictions under tension–tension and tension–compression conditions; however, the Drucker–Prager function seems to perform better than the von Mises function under biaxial compression.

3.2. *Evaluation based on the triaxial test data*

There is a general shortage of triaxial test data reported in the literature. Most of the existing triaxial tests are performed with large confining pressure for the purpose of examining the effect of hydrostatic pressure on concrete fracture strength. Thus, the reported results for triaxial states of stress are usually limited to triaxial compression tests. For the purpose of comparison, two sets of test data reported by Linse and Aschl (1976), and Palaniswamy and Shah (1974) are selected. The same loading functions used for biaxial conditions are considered here.

Based on Linse *et al.*'s data, τ/f'_c curves are plotted in Fig. 6. Considerable scattering is exhibited by the von Mises function, and to a lesser degree by the Drucker–Prager function. However, both loading functions give τ much higher values at fracture than the uniaxial compressive strength f'_c. Thus, both functions are not suitable for modeling triaxial concrete behavior under large confining pressure.

For the Hsieh *et al.* and the Willam–Warnke functions, the τ/f'_c values do not exceed 1.0 at failure and the hardening rates exhibit much less scatter than for the von Mises

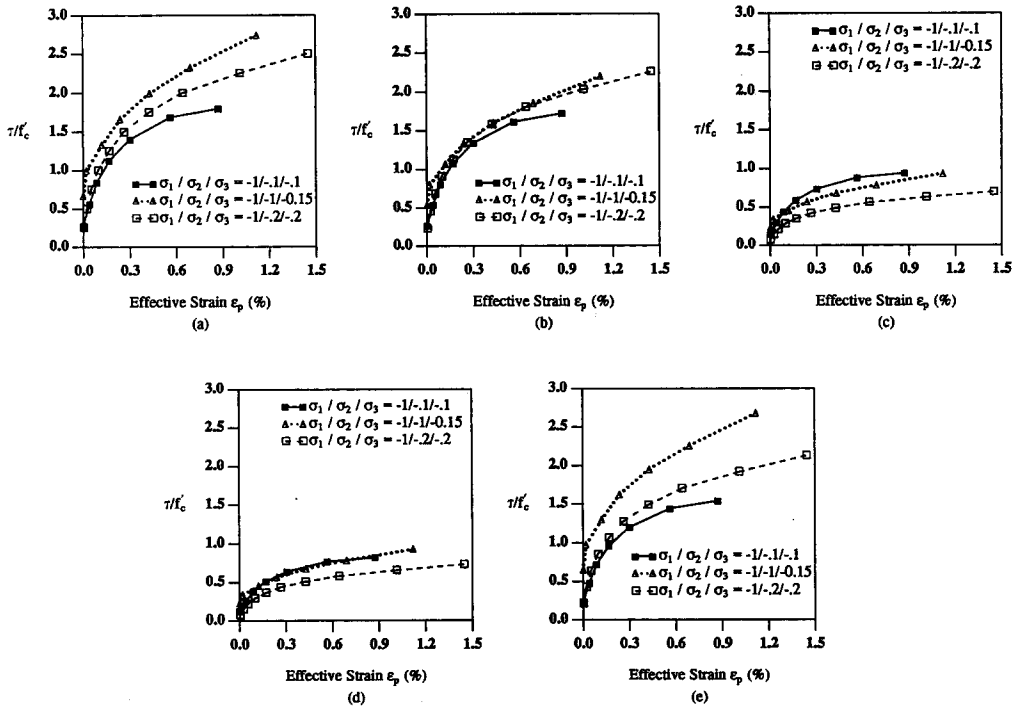

Fig. 6. Triaxial hardening parameter for different choices of loading functions based on Linse data: (a) von Mises, (b) Drucker–Prager, (c) Hsieh–Ting–Chen, (d) Willam–Warnke, and (e) Bresler–Pister.

and Drucker–Prager functions. The Bresler–Pister functions exhibit essentially the same characteristics as the von Mises functions and are not suitable for triaxial conditions.

The τ/f'_c vs ε_p curves for all five loading functions, based on test results of Palaniswamy *et al.*, are also studied. Similar conclusions are obtained.

Based on the above comparison using two different sets of triaxial data, it can be concluded that under large confining pressures, the Hsieh *et al.* and Willam–Warnke functions appear to be more suitable and the von Mises, Drucker–Prager and Bresler–Pister functions seem to be inappropriate for concrete modeling under these stress conditions.

3.3. *Modified von Mises and Drucker–Prager functions*

To illustrate that the scatter of the hardening rates for the von Mises and Drucker–Prager functions is due to the large confining pressure, the following simple form of the modified von Mises function is proposed by adding a mean stress correction factor:

$$\frac{\sqrt{3J_2}}{1-r\dfrac{\sigma_m}{f'_c}}-\tau=0, \tag{17}$$

where $r = 1$ when all the three principal stresses are compressive and $r = 0$ otherwise.

The Drucker–Prager function can also be modified in a similar manner:

$$\frac{\alpha I_1+\beta\sqrt{J_2}}{1-r\dfrac{\sigma_m}{f'_c}}-\tau=0. \tag{18}$$

Hardening parameters based on the modified von Mises and Drucker–Prager functions

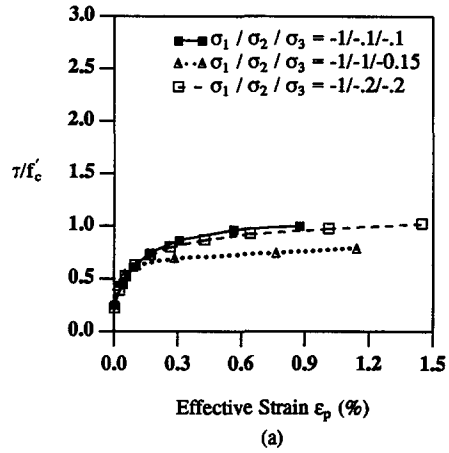

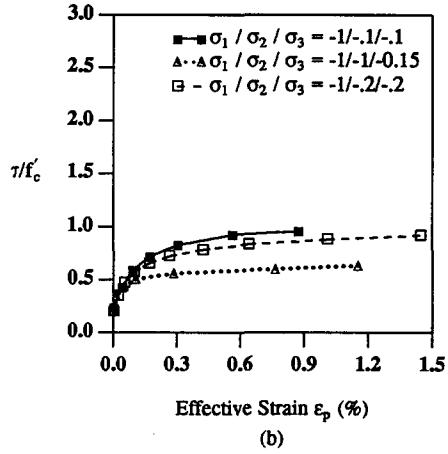

Fig. 7. Triaxial hardening parameter based on Linse data for (a) modified von Mises, and (b) modified Drucker–Prager.

are plotted in Fig. 7. For the two sets of data by Linse *et al.* and Palaniswamy *et al.*, the hardening curves exhibit less scatter than in the original functions. Moreover, the values of τ over f'_c are generally under 1.0.

To verify the validity of the modified von Mises, modified Drucker–Prager, Hsieh–Ting–Chen four parameter and Willam–Warnke five parameter functions, analytical stress–strain responses are obtained and then compared with the test results by Linse *et al.* Due to the presence of large volumetric strains under the confining pressure, the previously selected hardening function of eqn (15) appears to overestimate the hardening behavior of concrete under this condition, as seen in Fig. 8. A different hardening function is proposed for these conditions:

$$\frac{\tau}{f'_c} = 1.0 - 0.75\, e^{-175\varepsilon_p} \tag{19}$$

and the corresponding hardening rate is then

$$H = \frac{\partial \tau}{\partial \varepsilon_p} = 131 f'_c\, e^{-175\varepsilon_p}. \tag{20}$$

Figure 9 shows the predicted stress–strain response under triaxial stress conditions

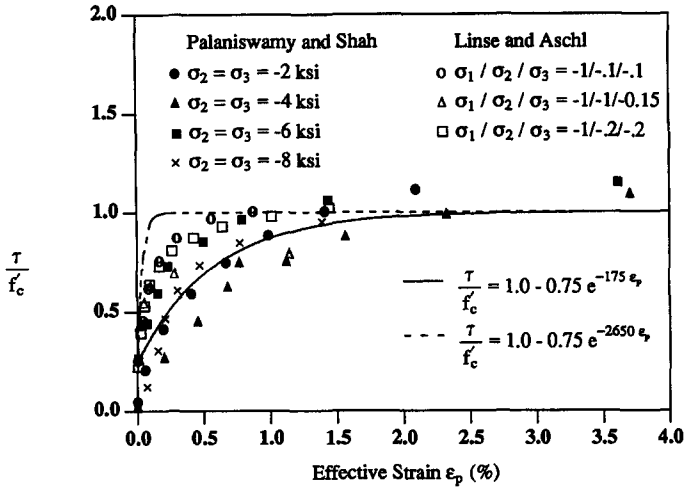

(a)

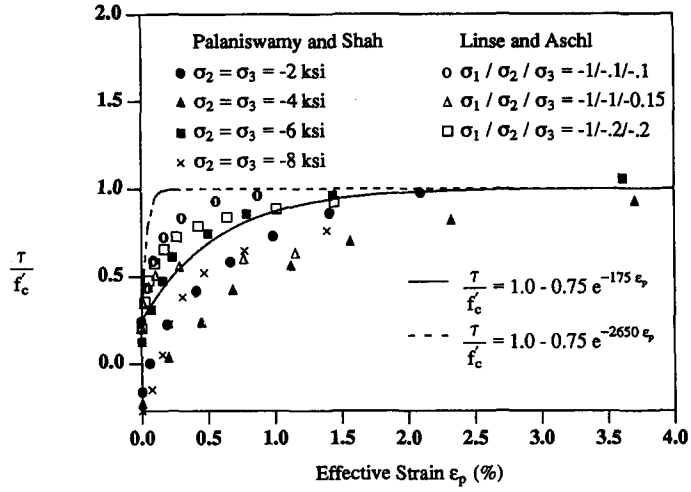

(b)

Fig. 8. Triaxial hardening parameter based on two sets of triaxial data: (a) modified von Mises and (b) modified Drucker–Prager.

compared to the experimental data of Linse *et al.* Based on these results, it appears that none of the considered loading functions is able to accurately predict the concrete behavior under these conditions. The modified von Mises and Drucker–Prager functions reasonably predict the major principal compressive strains, but greatly overestimate the tensile strain values for the stress ratios $\sigma_1/\sigma_2/\sigma_3$ of $-1/-0.1/-0.1$ and $-1/-0.2/-0.2$. For the stress ratio case of $-1/-1/-0.15$, compressive strains are underestimated, while tensile strains are overestimated. The Hsieh–Ting–Chen and Willam–Warnke yield similarly poor results.

From the above results, it appears that in the presence of high confining pressure, it is difficult to model the hardening behavior of concrete using a single hardening parameter as a function of the total effective plastic strain. Since large volumetric strains dominate the behavior of concrete under high confining pressure, hardening functions based on total effective plastic strain may overestimate the hardening capacity of concrete. Considering the hydrostatic and deviatoric effective strain components separately appears to be a promising alternative to employing a single hardening function based on the total effective plastic strain.

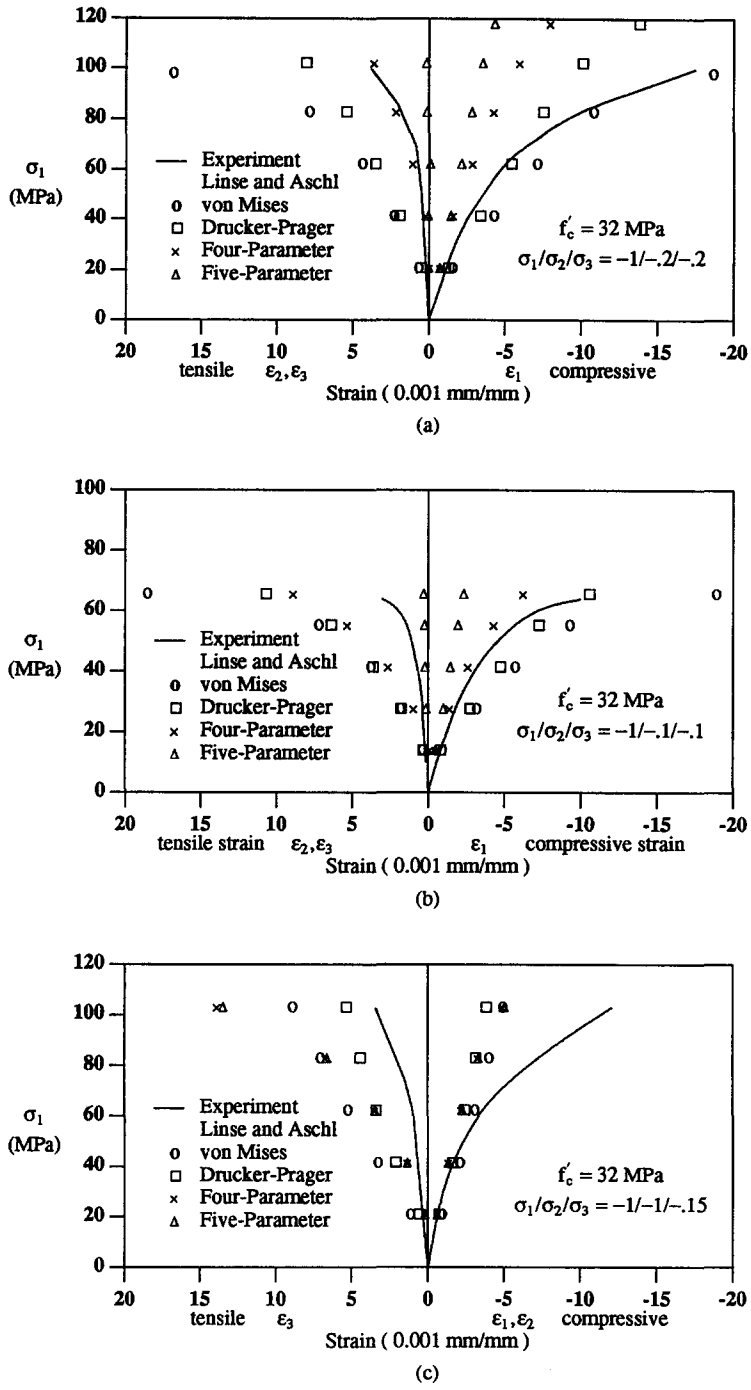

Fig. 9. Triaxial compressive stress–strain behavior under three different stress ratios.

4. FINITE ELEMENT ANALYSIS

The performance of the loading functions under homogeneous deformations has been examined in detail. In the following, we examine their applicability to a finite element analysis of a general structure. It has often been argued that the selection of a plasticity model makes little difference as far as load-deformations and ultimate strength of concrete structures are concerned. While it is well recognized that post-cracking behavior plays a

major role in the response of concrete structures, accurate prediction of stresses prior to cracking is indispensable and has a significant effect on the overall response of the structure.

Our comparative study includes the prediction of the response of the standard split tension test of a plain concrete cylinder, and a reinforced concrete slab subjected to uniform distributed loading.

Modeling reinforced concrete for finite element analysis is an exceedingly complex task. In addition to the constitutive modeling prior to fracture, modeling of the post-cracking behavior is also necessary in order to be able to predict the response of concrete structures. The algorithm must have the capability of efficiently handling the long sequence of behavior changes and material nonlinearities. Furthermore, in many concrete structures such as slabs, it is necessary to include the geometry changes due to large deflection. Thus, the selection of a proper finite element code for analysis is of primary importance. In the present study, two finite element codes are adopted for the implementation of the material models. The first code is used for the analysis of planar and axisymmetric structures, while the second code is employed in the analysis of plate and shell structures. The basic finite element codes are based on an algorithm originally used in codes STRAW and SADCAT developed at Argonne National Laboratory. The algorithm was recoded as STRAWP and CBS-1 at Purdue University with considerable modifications. Complete concrete models are implemented for the present study.

The solution algorithm in both codes is implemented for transient dynamic analysis. Explicit time integration based on central difference is used to find the time histories of the nodal acceleration, velocity and displacement. The technique requires relatively small core storage and less computational effort by avoiding the assemblage of large global matrices and a lengthy iterative process. To ensure numerical stability, a small time increment needs to be used. However, this is hardly a disadvantage due to the inherent nonlinearities and discontinuities in the plasticity and crack models. Static solutions can be obtained by considering a slow ramp loading history and incorporating a dynamic relaxation procedure.

For the large deflection formulation, the co-rotational approach is employed. One of the main advantages of the approach is that the deformation written in convected and body coordinates can be approximated by using an infinitesimal strain theory. Thus, the material models can be applied without the need of modifications.

For the post-fracture stress–strain relationship, an anisotropic elastic model is adopted. The concrete fracture is categorized into three different modes; namely, cracking, crushing and a mixed mode. Stresses are released according to the identified failure mode.

Four of the plasticity models evaluated in the preceding section are implemented; namely, the von Mises, Drucker–Prager, Hsieh–Ting–Chen and Willam–Warnke models. In the case of the von Mises and Drucker–Prager models, the Hsieh–Ting–Chen failure criterion is proposed to define the ultimate state of stress and the initiation of cracks.

In the following, the results of the numerical analysis of two benchmark problems are presented and compared to the experimental data where it applies.

4.1. *Split tension test of a plain concrete cylinder*

The split tension test is a standard method for determining the tensile strength of concrete. The test is performed on a concrete cylinder laid horizontally between two loading platens of the testing machine. The cylinder is compressed gradually until it splits across the vertical diameter of the cross-section. Details of the test specimen as well as the finite element mesh are shown in Fig. 10.

Figure 11 plots the load vs vertical displacement curve just under the loading strip. The horizontal and vertical stress distributions along the vertical diameter are shown in Fig. 12. As anticipated, the von Mises and Drucker–Prager models yield essentially the same response. On the other hand, both the Hsieh–Ting–Chen and the Willam–Warnke models predict a similarly higher failure load. Examining the stress distribution near fracture shown in Fig. 12(a), it can be seen that the latter two models predict lower tensile stresses at the center of the cylinder due to their softer stress–strain responses under tension–tension and tension–compression states of stress. Judging by the load–displacement plot, the behavior of a split tension test appears to be dominated by the elastic response and cracking.

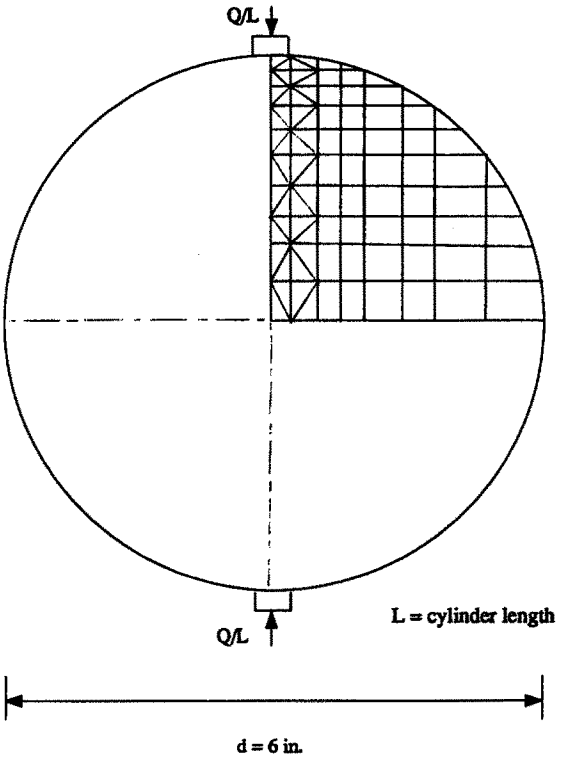

Fig. 10. A split tension test sample.

It seems reasonable to assume that the plastic (or micro-cracking) behavior would not affect the overall response and in particular, the failure load significantly. Our analysis has shown that this assumption can lead to large discrepancies. Since the local tensile stress values dominate the crack initiation and hence the crack propagation through the concrete medium, an inaccurate tensile stress prediction as the result of poor stress–strain modeling may lead to large discrepancies.

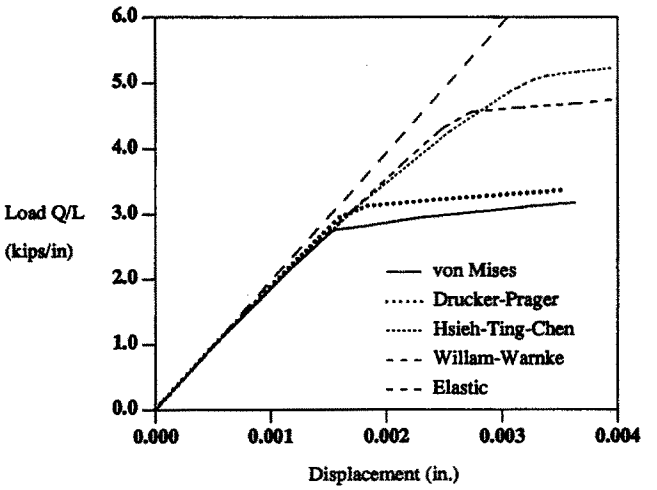

Fig. 11. Comparison of load–displacement responses of split tension specimen for various models.

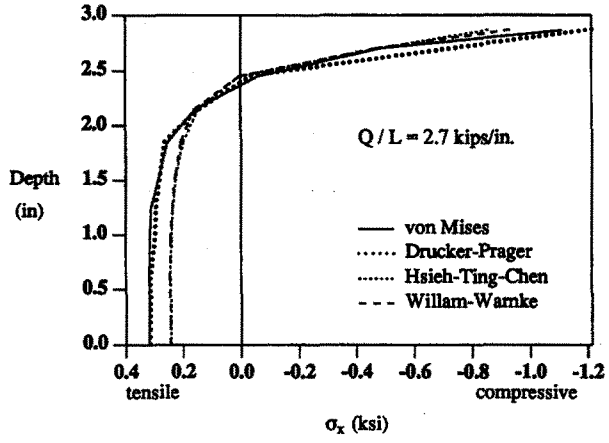

(a)

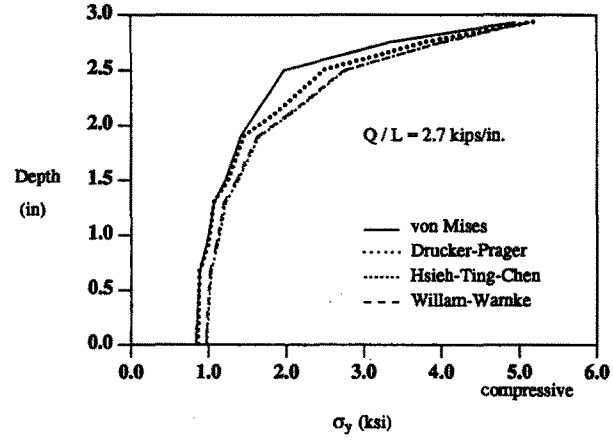

(b)

Fig. 12. Comparison of vertical and horizontal stress distributions of split tension specimen for various models.

4.2. *Reinforced concrete slab under uniform loading*

The analysis of a reinforced concrete slab, tested by Taylor *et al.* (1966), is carried out using the von Mises, Drucker–Prager and Hsieh–Ting–Chen models. The slab is simply supported on all four edges. Details of the reinforcement and dimensions of the slab are shown in Fig. 13. We did not implement the Willam–Warnke model in our plate-shell code due to the complexity of the model. However, we anticipate its behavior to be quite similar to the Hsieh–Ting–Chen model.

In the present analysis, it is noted that tension stiffening effects are not accounted for. Figure 14 illustrates experimental and predicted deflection curves. The von Mises and Drucker–Prager models yield an almost identical response and a better agreement with the experimental results. Near failure, the Drucker–Prager model exhibits slightly higher stiffness than the von Mises model. This is because the von Mises model does not account for the increase in strength under biaxial compression. The Hsieh–Ting–Chen model predicts a substantially higher failure load than the von Mises and Drucker–Prager models. This discrepancy is attributed to the far too soft response exhibited by the Hsieh–Ting–Chen model in the tension–tension and tension–compression zones. As shown in the earlier part of this study, the model greatly underestimates the tensile stresses under these loading

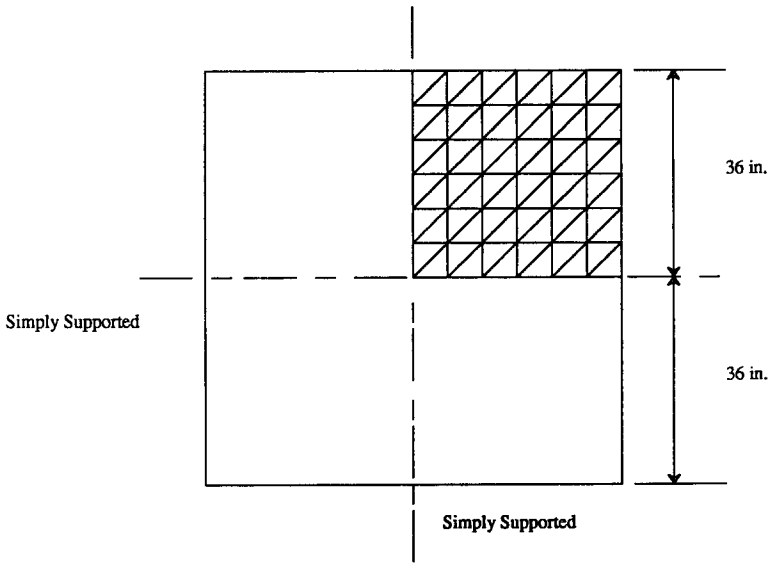

(a)

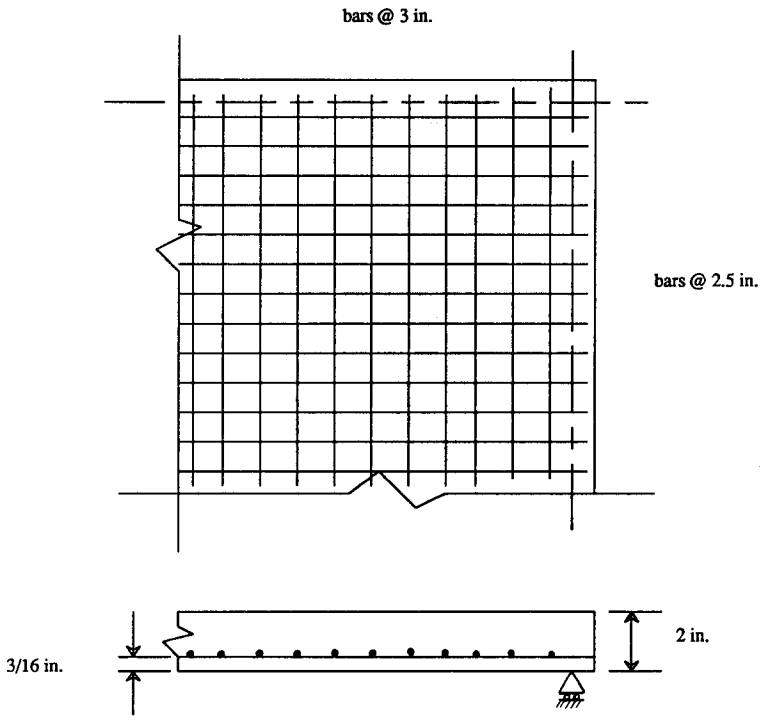

(b)

Fig. 13. A simply-supported reinforced concrete slab subjected to uniform loads (Taylor slab S1): (a) finite element model and (b) test sample.

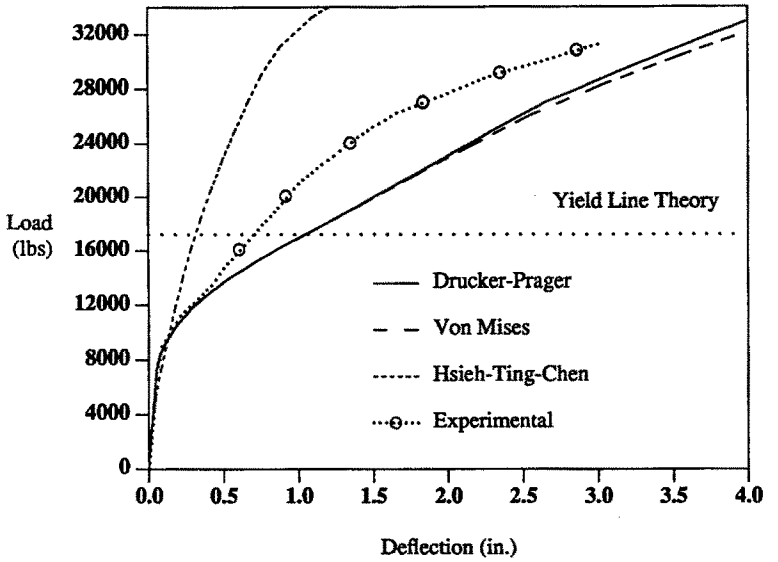

Fig. 14. Load–central deflection curves for Taylor slab S1.

conditions. As a result, tensile crack initiation, which controls the failure of the slab, is delayed and a higher failure load is predicted.

5. CONCLUSION

The loading functions of several commonly adopted plasticity-based concrete models were evaluated in this study. It was shown that under biaxial stress conditions, the Hsieh–Ting–Chen, and Willam–Warnke and the Bresler–Pister models had widely varying hardening rates. When uniaxial compression test data were used to characterize concrete hardening, the above models resulted in a stiffer response in biaxial compression state of stress, and a softer response in tension–tension and tension–compression states. On the other hand, the von Mises and Drucker–Prager functions exhibited an almost uniform hardening rate under all biaxial loading conditions. Both functions achieved better accuracy under all biaxial conditions. Based on these results, it can be concluded that the usual assumption of employing yielding and loading functions that have the same functional form as the fracture criterion places considerable limitations on the development of concrete models. It was found that models based on this assumption, not only required a more intensive computational effort, but also yielded poor predictions under various loading conditions.

Under triaxial compression states of stress, none of the considered functions was able to accurately and consistently predict the behavior of concrete. Because of the presence of high volumetric strains under high confining pressure, it is necessary to consider the volumetric and distortional behaviors separately when determining the hardening rate of concrete under these conditions. For general triaxial states of stress, further experimental data are needed to serve as a basis for the development and verification of material models.

The significance of the loading functions on the prediction of the response of reinforced concrete structures was also illustrated by two example problems. Accurate predictions of the stress–strain relationships appeared to be of critical importance. The overall response and failure can be greatly affected by the choice of the yield criterion and loading functions.

Acknowledgements—The topic was first suggested by Dr A. H. Marchertąs of Argonne National Laboratory during ECT's visit at Argonne. Preliminary study was initiated by ECT with Dr Y. Takahashi of Tokyo University, Japan at Argonne in 1983. Due to the extensive amount of code development required to complete the study, the overall study spanned seven years. Dr Saha developed code STRAWP for planar concrete structures and carried out the first portion of the evaluation. Subsequently, a former graduate student, K. Vajarasathira and Dr Labbane reprogrammed the computer code and implemented CBS-1 for concrete plate and shell structures. All the material

data were re-examined. We are deeply indebted to Drs J. Kennedy and A. H. Marchertas for making STRAW and SADCAT available to Purdue University, so the codes STRAWP and CBS-1 could be developed. We would also like to thank our colleagues Professors C. D. Sutton and M. Yener of Purdue University for many valuable suggestions during the course of this study.

REFERENCES

Bresler, B. and Pister, K. S. (1958). Strength of concrete under combined stresses. *J. Am. Concr. Inst.* **55,** 321–345.

Drucker, D. C. and Prager, W. (1952). Soil mechanics and plasticity analysis of limit design. *Q. Appl. Mech.* **10,** 157–165.

Hsieh, S. S., Ting, E. C. and Chen, W. F. (1982). A plastic-fracture model for concrete. *Int. J. Solids Structures* **18,** 181–197.

Kupfer, H., Hilsdorf, H. K. and Rush, H. (1969). Behavior of concrete under biaxial stresses. *J. Am. Concr. Inst.* **66,** 656–666.

Labbane, M., Saha, N. K. and Ting, E. C. (1991). Evaluation of plasticity-based models for concrete. *Struct. Eng. Rep, CE-STR-91-18, Purdue University.*

Linse, D. H. and Aschl, H. (1976). Tests on the behavior of concrete under multiaxial stresses. Technical University of Munich, Department of Reinforced Concrete Report.

Palaniswamy, R. and Shah, S. P. (1974). Fracture and stress–strain relationship of concrete under triaxial compression. *ASCE J. Struct. Div.* **100,** 901–916.

Tasuji, M. E., Slate, F. O. and Nilson, A. H. (1978). Stress–strain response and fracture of concrete in biaxial loading. *J. Am. Concr. Inst.* **75,** 306–312.

Taylor, R., Maher, D. R. H. and Hayes, B. (1966). Effect of the arrangement of reinforcement on the behavior of reinforced concrete slabs. *Mag. Concrete Research* **98,** 85–94.

Willam, K. J. and Warnke, E. P. (1974). Constitutive models for the triaxial behavior of concrete. *Int. Assoc. Bridge Struc. Eng. Sem. Concr. Struc. Subjected to Triaxial Stresses.*